system. As pointed out by Read and Margerum,[25] if the donor is unrestricted and able to move easily out of the first coordination sphere, the presence of acid has little effect. However, if the movement of the donor away from the metal ion is hindered in some way, acid can enhance the rate of dissociation. The restrictions holding the donor in the first coordination sphere imposed by the 6,5,6-membered chelate rings are larger than those imposed by the 6,6,6-membered chelate rings. Consequently, ring opening is easier for the 6,6,6-membered rings, making the direct protonation pathway less important.

For copper(II) complexes of macrocyclic tetraamines, the restrictions imposed by the macrocyclic ligand hold the donor atoms strongly in the first coordination sphere. Consequently, the direct protonation pathway becomes very important for the dissociation reactions of these complexes; therefore, the ratio of the rate constant of dissociation by the direct protonation pathway to the rate constant by the proton-assisted pathway for the macrocyclic ligand complex in planar coordination is extremely large.[3,5]

The results tabulated in Table II indicate that the ratios of k_4/k_3 for the complexes with the 6,6,6-membered ring system are slightly larger than those with the 6,5,6-membered ring system. This is attributed to the difference in the distance between the uncoordinated amino group and the metal ion in III (Figure 3). The additional methylene group in the complex with the 6,6,6-membered ring system increases the distance between the released amino group and the metal ion; thus, protonation of the released amino group (III → VI) is faster for the complex with the 6,6,6-membered ring system.

The values of the ratios k_{-2}/k_3 and k_{-2}/k_4 tabulated in Table II indicate that these ratios for the complexes with the 6,5,6-membered ring system are much larger than those with the 6,6,6-membered ring system. This is related to two factors: (1) the ring strain in linked consecutive rings and (2) the proximity effect. The ring strains in linked consecutive 6-membered rings are very large;[29] thus, the formation of the second Cu–N bond (III → V in Figure 3) for the complex with a center 6-membered ring is much slower than that with a 5-membered ring. In addition, the proximity effect also favors the formation of the center 5-membered chelate ring.[2] Consequently, the ratios k_{-2}/k_3 and k_{-2}/k_4 for the complexes with the 6,5,6-membered ring system are much larger than those with the 6,6,6-membered ring system.

Acknowledgment. The support of the Chemistry Research Center, National Science Council of the Republic of China, under Grants NSC75-0208-M007-04 and NSC76-0208-M007-66 is gratefully acknowledged.

(29) Wang, B.; Chung, C.-S. *J. Chem. Soc., Dalton Trans.* **1982**, 2565–2566.

Contribution from the Department of Chemistry,
Texas A&M University, College Station, Texas 77843

Electrochemical Oxidation of Hydroxide Ion in Acetonitrile and Its Facilitation by Transition-Metal Complexes

Paul K. S. Tsang, Pablo Cofrê, and Donald T. Sawyer*

Received February 20, 1987

The oxidation of hydroxide ion and phenoxide ion in acetonitrile has been characterized by cyclic voltammetry at glassy-carbon electrodes. In the presence of transition-metal complexes $M^{II}L^{2+}$ [M = Mn, Fe, Co, Ni; L = $(OPPh_3)_4$, (2,2'-bipyridine)$_3$] and metalloporphyrins M(por) [M = Mn(III), Fe(III), Co(II); por = 5,10,15,20-tetraphenylporphinato(2–), 5,10,15,20-tetrakis-(2,6-dichlorophenyl)porphinato(2–)] the oxidation potentials for $^-$OH and PhO$^-$ are shifted to less positive potentials. This is due to the stabilization of the oxy radical products ($^\bullet$OH and PhO$^\bullet$) via formation of a d–p (d^n–$^\bullet$OR) covalent bond. With excess $^-$OH relative to the metal complex, oxidation of $^-$OH is facilitated by an ECE mechanism [ML($^-$OH) $\xrightleftharpoons{-e^-}$ ML($^\bullet$OH) $\xrightarrow{^-OH}$ ML(O$^\bullet$$^-$)(OH$_2$) $\xrightleftharpoons{-e^-}$ ML(O$^{2\bullet}$)(OH$_2$)].

The electrochemical oxidation of $^-$OH in aqueous[1] and aprotic[2-4] solvents along with the chemical reactivity of $^-$OH with various substrates (e.g., CCl_4,[5] anthraquinone,[6] and $Fe^{III}(TPP)^+$ in pyridine[7]) indicates that $^-$OH is an effective one-electron reductant. Other investigations have shown that the oxidations of metal–catechol[8-10] and metal–dithiolate[11] complexes are ligand-centered rather than metal-centered. In the latter investigation ligand oxidation is facilitated via formation of a d–p covalent bond (from an unpaired p electron of oxidized ligand and an unpaired d electron of the transition-metal center).

These observations have prompted us to examine the electrochemical oxidation of $^-$OH and the effect of transition-metal complexes upon the electron-transfer potential. A specific goal has been to establish that the activated iron–oxygen intermediates of cytochrome P-450, peroxidase, and catalase involve 0-valent and −1-valent oxygen rather than iron(IV) or porphyrin radical (on the basis of their respective redox thermodynamics).

Experimental Section

Equipment. Cyclic voltammetry and controlled-potential electrolysis were accomplished with a Bioanalytical Systems Model CV-27 and a Houston Instruments Model 200·XY recorder. The electrochemical measurements were made with a microcell assembly (10-mL capacity) that was adapted to use a glassy-carbon working electrode, a platinum-wire auxiliary electrode (contained in a glass tube with a medium-porosity glass frit and filled with a concentrated solution of supporting electrolyte), and a Ag/AgCl reference electrode (filled with aqueous tetramethylammonium chloride solution and adjusted to 0.000 V vs SCE)[12] with a solution junction via a glass tube closed with a cracked-glass bead that was contained in a luggin capillary. A platinum-mesh working electrode and a platinum-wire auxiliary electrode were used for the controlled-potential electrolysis experiments.

Chemicals and Reagents. Acetonitrile (MeCN), "distilled-in-glass" grade (0.004% H_2O) from Burdick and Jackson, was used without further purification. Tetraethylammonium perchlorate (TEAP) was vacu-

(1) (a) Schwarz, H. A.; Godson, R. W. *J. Phys. Chem.* **1984**, *88*, 3643–3647. (b) Hoare, J. P. In *Standard Potentials in Aqueous Solution*; Bard, A. J., Parsons, R., Jordan, J., Eds.; Dekker: New York, 1985; pp 49–66.
(2) Goolsby, A. D.; Sawyer, D. T. *Anal. Chem.* **1968**, *40*, 83–86.
(3) Simonson, L. A.; Murray, R. W. *Anal. Chem.* **1975**, *47*, 290–294.
(4) Sawyer, D. T.; Doub, W. H., Jr.; Marsden, P. J. *Anal. Chem.* **1976**, *48*, 1628–1632.
(5) Roberts, J. L., Jr.; Calderwood, T. S.; Sawyer, D. T. *J. Am. Chem. Soc.* **1983**, *105*, 7691–7696.
(6) Roberts, J. L., Jr.; Sugimoto, H.; Barrette, W. C., Jr.; Sawyer, D. T. *J. Am. Chem. Soc.* **1985**, *107*, 4556–4557.
(7) Srivatsa, G. S.; Sawyer, D. T. *Inorg. Chem.* **1985**, *24*, 1732–1734.
(8) Jones, S. E.; Leon, L. E.; Sawyer, D. T. *Inorg. Chem.* **1982**, *21*, 3692–3698.
(9) Bodini, M. E.; Copia, G.; Robinson, R.; Sawyer, D. T. *Inorg. Chem.* **1983**, *22*, 126–129.
(10) Haga, M.-A.; Rodsworth, E. S.; Lever, A. B. P. *Inorg. Chem.* **1986**, *25*, 447–453.
(11) Sawyer, D. T.; Srivatsa, G. S.; Bodini, M. E.; Schaefer, W. P.; Wing, R. M. *J. Am. Chem. Soc.* **1986**, *108*, 936–942.
(12) Sawyer, D. T.; Roberts, J. L., Jr. *Experimental Electrochemistry for Chemists*; Wiley: New York, 1974; pp 44–46, 144–145, 336–339.

0020-1669/87/1326-3604$01.50/0

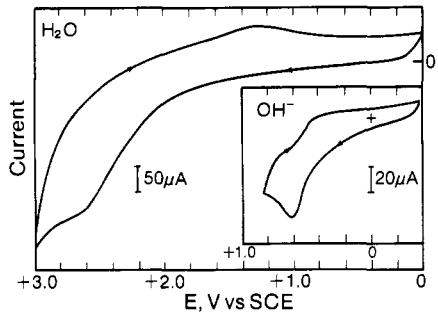

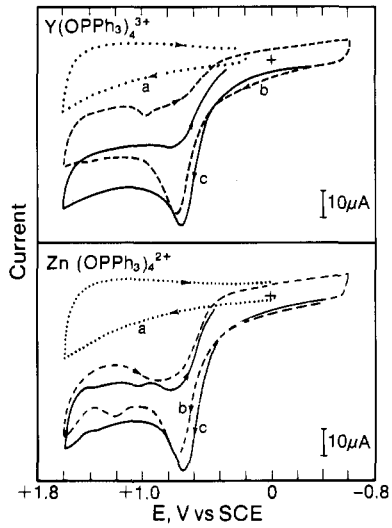

Figure 1. Cyclic voltammograms in MeCN (0.1 M TEAP) of (top) 3 mM H_2O and 5 mM tetrabutylammonium hydroxide ((TBA)OH) in methanol, (middle) (TBA)OH in the presence of $Y^{III}(OPPh_3)_4(ClO_4)_3$, and (bottom) (TBA)OH in the presence of $Zn^{II}(OPPh_3)_4(ClO_4)_2$ [scan rate 0.1 V s^{-1}; glassy-carbon electrode (GCE) (area 0.07 cm^2); SCE +0.24 V vs NHE]: curve a, scan for 1.0 mM metal complex; curve b, first scan after addition of 4 mM (TBA)OH; curve c, scan after complete precipitation (ca. 2 min).

um-dried for 24 h prior to use. Tetrabutylammonium hydroxide [$(Bu_4N)OH$] was obtained from Aldrich as a 25% solution in methanol, and its concentration was determined by acid–base titration. A solution of phenoxide ion was prepared by the addition of an equimolar MeOH solution of $(Bu_4N)OH$ to a solution of PhOH (H_2O was produced upon neutralization). All other solvents and chemicals were reagent grade and were used as received.

Preparation of Complexes. The complexes $M^{II}(OPPh_3)_4(ClO_4)_2$[13,14] (M = Mn, Fe, Co, Ni, Zn), $Y^{III}(OPPh_3)_4(ClO_4)_3$[13,14], $M^{II}(bpy)_3(ClO_4)_2$[15] (M = Mn, Fe, Co, Ni, Zn; bpy = 2,2′-bipyridine), $(TDCPP)Fe^{III}(ClO_4)$[16,17] [TDCPP = 5,10,15,20-tetrakis(2,6-dichlorophenyl)-porphyrinato(2−)], and $(TPP)Mn^{III}(ClO_4)$[18] [TPP = 5,10,15,20-tetraphenylporphinato(2−)] were prepared by literature methods. The preparation of $(TPP)Fe^{III}(ClO_4)$ used the procedure for the synthesis of (octaethylporphinato)iron(III) perchlorate.[19]

Results

Figure 1 illustrates the electrochemical oxidation of H_2O ($E_{1/2}$ = +2.43 V vs SCE) and ^-OH (+0.55 V vs SCE) at a glassy-carbon electrode in acetonitrile.[20] In the presence of transition-metal complexes with filled d subshells ($Y^{III}(OPPh_3)_4^{3+}$ or $Zn^{II}(OPPh_3)_4^{2+}$) the oxidation of ^-OH occurs at a slightly more positive potential than that for free ^-OH (Figure 1 and Table I). Curve a (dotted line) of Figure 1 illustrates the cyclic voltammogram for 1.0 mM $Y^{III}(OPPh_3)_4^{3+}$ prior to addition of ^-OH. The initial cyclic voltammogram (curve b, dashed line) immediately after the addition of excess base (4 mM) exhibits a well-defined oxidation peak at a more positive potential than the cyclic voltammogram of free ^-OH ($E_{1/2}$ = +0.63 V vs SCE). Within 2 min the metal complex precipitates completely, which is confirmed by an oxidation for residual free ^-OH (curve c, solid line).

The oxidation of ^-OH in the presence of transition-metal complexes with partially filled d subshells [$Mn^{II}(OPPh_3)_4^{2+}$, $Fe^{II}(OPPh_3)_4^{2+}$, $Co^{II}(OPPh_3)_4^{2+}$, and $Ni^{II}(OPPh_3)_4^{2+}$] is illustrated

Table I. Oxidation Potentials of 4–5 mM ^-OH in the Presence of Transition-Metal Complexes

	$E_{1/2}$, V vs SCE[a]					
	^-OH[b]	Zn	Ni	Co	Fe	Mn
^-OH	+0.55					
$M^{II}(OPPh_3)_4^{2+}$[c]		+0.63	−0.05	−0.09	+0.08[d]	+0.27
$M^{II}(bpy)_3^{2+}$[c]		+0.66	−0.03	+0.02	+0.28	+0.33

[a] $E_{1/2} = E_{p/2} + 0.03$; Bard, A. J.; Faulkner, L. R. *Electrochemical Methods*; Wiley: New York, 1980; pp 236–243. [b] $E_{1/2}$ for 1.5 mM ^-OH is +0.35 V vs SCE; the difference is due to increased levels of water and uncompensated *iR*. [c] 1 mM metal complex and 4 mM $(Bu_4N)OH$. [d] 1 mM metal complex, 10 mM $OPPh_3$, and 4 mM $(Bu_4N)OH$.

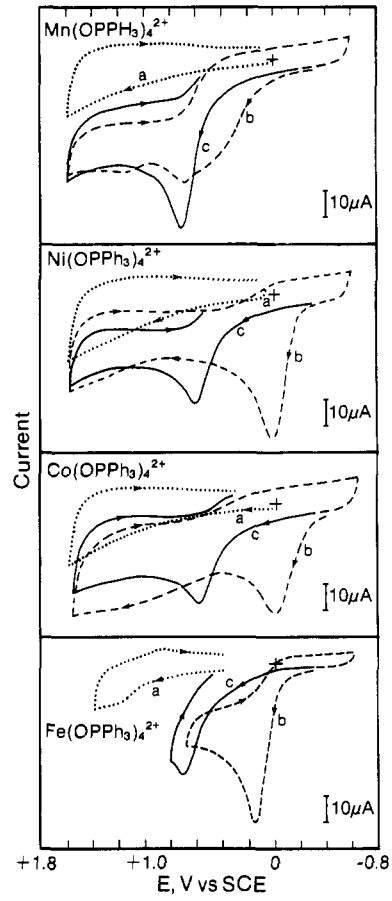

Figure 2. Cyclic voltammograms in MeCN (0.1 M TEAP) of (TBA)OH in the presence of $M^{II}(OPPh_3)_4(ClO_4)_2$ complexes (M = Mn, Ni, Co, Fe) [scan rate 0.1 V s^{-1}; GCE (area 0.07 cm^2)]: curve a, scan for 1.0 mM metal complex; curve b, first scan after addition of 4 mM (TBA)OH; curve c, scan after complete precipitation (ca. 10 min.). For the $Fe^{II}(OPPh_3)_4^{2+}$ experiment excess $OPPh_3$ (10 mM) was also added to reduce the rate of precipitation.

(13) Cotton, F. A.; Bannister, E. *J. Chem. Soc.* **1960**, 1873–1877.
(14) Bannister, E.; Cotton, F. A. *J. Chem. Soc.* **1960**, 1878–1882.
(15) Burstall, F. H.; Nyholm, R. S. *J. Chem. Soc.* **1952**, 3570–3579.
(16) Badger, G. M.; Jones, R. A.; Laslete, R. L. *Aust. J. Chem.* **1964**, *17*, 1028.
(17) Woon, T. C.; Shirazi, A.; Bruice, T. C. *Inorg. Chem.* **1986**, *25*, 3845–3846.
(18) Hill, C. L.; Williamson, M. M. *Inorg. Chem.* **1985**, *24*, 2836–2841.
(19) Dolphin, D. H.; Sams, J. R.; Tsin, T. B. *Inorg. Chem.* **1977**, *16*, 711–713.

(20) The SCE is +0.24 V vs NHE.

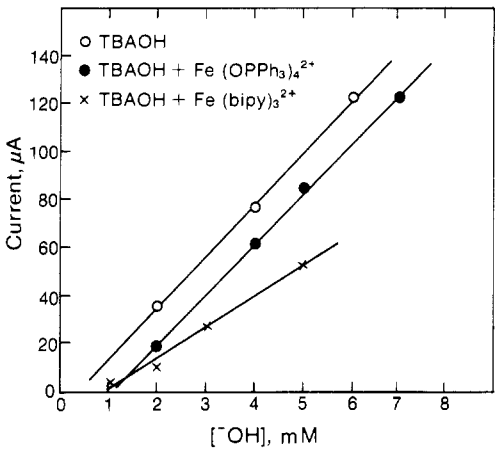

Figure 3. Plots of the anodic voltammetric peak current for ^-OH as a function of [(TBA)OH] in MeCN (0.1 M TEAP) [scan rate 0.1 V s^{-1}; GCE (area 0.07 cm^2)]: (○) free (TBA)OH; (●) (TBA)OH in the presence of 1 mM $Fe^{II}(OPPh_3)_4(ClO_4)_2$ and 10 mM $OPPh_3$; (×) (TBA)OH in the presence of 1 mM $Fe^{II}(bpy)_3(ClO_4)_2$ and 9 mM bpy. Excess ligand was used to slow down the precipitation process and improve resolution of the oxidation peak.

by Figure 2, with curve a for the metal complex in the absence of ^-OH. Curve b [recorded immediately after the addition of excess ^-OH (4 mM) to the metal complex (1.0 mM)] indicates that ^-OH is oxidized at much less positive potentials than is free ^-OH. Subsequent voltage scans yield voltammograms with a decrease in the peak current for the less positive oxidation peak; precipitation of the metal hydroxide is complete within 10 min. When the ligand is 2,2′-bipyridine, similar behavior is observed. Table I summarizes the peak potentials for the oxidation of ^-OH in the presence of both series of transition-metal complexes. In the presence of iron(II) complexes the anodic peak current for metal-associated ^-OH increases linearly with its concentration (Figure 3). The slopes for oxidation of free ^-OH and for ^-OH in the presence of 1 mM $Fe^{II}(OPPh_3)^{2+}$ are essentially the same and twice that for ^-OH in the presence of 1 mM $Fe^{II}(bpy)_3^{2+}$.

Metal Porphyrins. Figure 4 illustrates cyclic voltammograms for $Zn^{II}(TPP)$ and for its 1:1 and 1:3 combinations with ^-OH. The 1:1 combination exhibits a new irreversible anodic peak ($E_{1/2}$ = +0.51 V vs SCE). With further addition of ^-OH another anodic peak appears that is due to free ^-OH ($E_{1/2}$ = +0.24 V). Although $Zn^{II}(TPP)$ is not completely soluble in MeCN,[21] the addition of ^-OH to $Zn^{II}(TPP)$ yields a clear solution.

The voltammetry for $Co^{II}(TPP)$ and for its 1:1 and 1:3 combinations with ^-OH is illustrated in Figure 5. Because $Co^{II}(TPP)$ is insoluble in MeCN,[21] the cyclic voltammogram of $Co^{II}(TPP)$ has been obtained by the addition of excess ^-OH to induce its dissolution. Subsequent neutralization with $HClO_4$ yields dissolved $Co^{II}(TPP)$.

Addition of ^-OH to $(TPP)Fe^{III}(ClO_4)$ in MeCN causes most of it to precipitate. However, its reduction by electrolysis to $Fe^{II}(TPP)$ prior to the addition of ^-OH permits anodic voltammograms to be recorded. This problem does not occur with the octachloro derivative $[(TDCPP)Fe^{III}(ClO_4)]$; the electrochemical oxidation of ^-OH in its presence is illustrated in Figure 6 [the irreversible reduction of Fe(II) to Fe(I) for $(TDCPP)Fe^{III}(ClO_4)$ occurs at −1.01 V vs SCE]. The addition of 1 equiv of ^-OH causes the Fe(III)/Fe(II) couple to shift to a more negative potential and results in the appearance of a new irreversible oxidation ($E_{1/2}$ = +1.09 V vs SCE). With the addition of excess ^-OH, the anodic voltammogram exhibits two new peaks ($E_{1/2}$ = −0.10 and +0.40 V).

The electrochemistry of $(TPP)Fe^{III}(ClO_4)$ and of its 1:1 and 1:3 combinations with PhO^- is illustrated in Figure 7. The addition of 1 equiv of PhO^- causes the Fe(III)/Fe(II) couple to shift to a more negative potential and results in a new anodic peak ($E_{1/2}$ = +0.91 V vs SCE). Further addition of PhO^- results in the appearance of an anodic peak for free PhO^- ($E_{1/2}$ = +0.09 V vs SCE).

(21) Solvents with better solvating properties were not used because they were more susceptible than MeCN to hydrolysis by ^-OH.

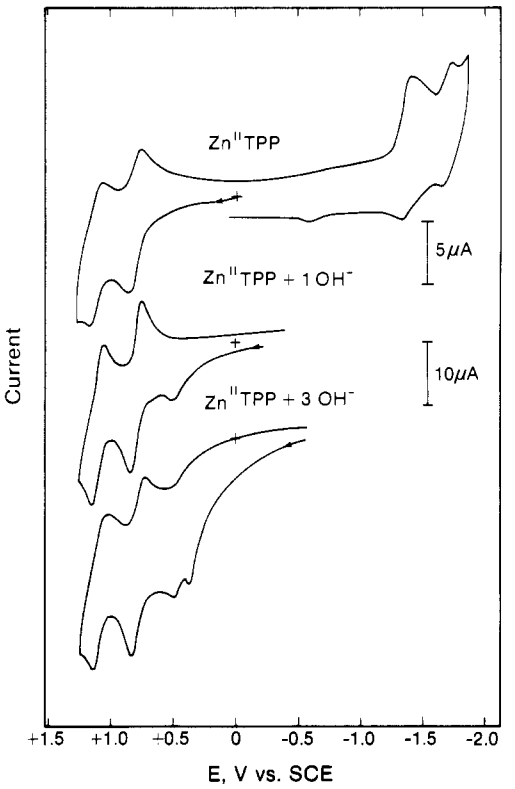

Figure 4. Cyclic voltammograms in MeCN (0.1 M TEAP) of (top) 0.7 mM $Zn^{II}(TPP)$; (middle) 0.7 mM $Zn^{II}(TPP)$ +1 equiv of (TBA)OH, and (bottom) 0.7 mM $Zn^{II}(TPP)$ + 3 equiv of (TBA)OH [scan rate 0.1 V s^{-1}; GCE (area 0.062 cm^2)].

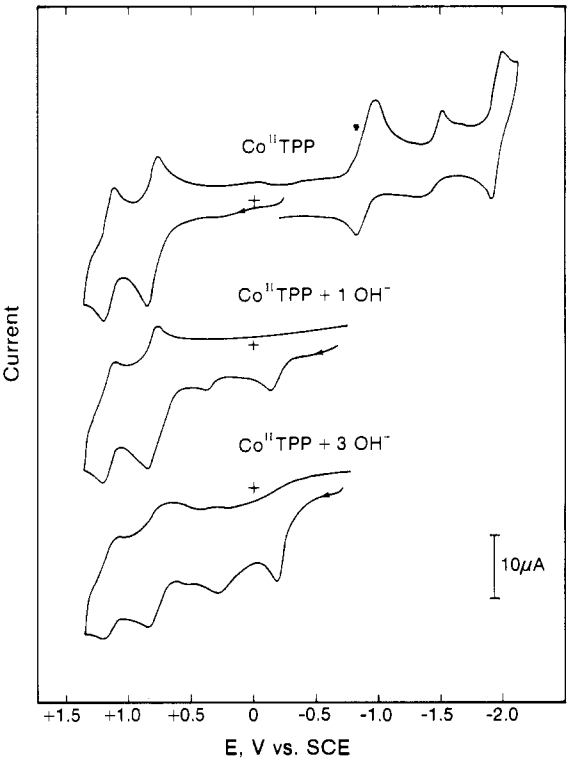

Figure 5. Cyclic voltammograms in MeCN (0.1 M TEAP) of (top) 0.6 mM $Co^{II}(TPP)$ + 3 equiv of (TBA)OH + 3 equiv of $HClO_4$, (middle) 0.6 mM $Co^{II}(TPP)$ + 3 equiv of (TBA)OH + 2 equiv of $HClO_4$, and (bottom) 0.6 mM $Co^{II}(TPP)$ + 3 equiv of (TBA)OH [scan rate 0.1 V s^{-1}; GCE (area 0.062 cm^2)].

Table II. Oxidation Potentials of ^-OH and PhO^- in the Presence of Metalloporphyrins

	$E_{1/2}$, V vs SCE				
	^-OH			PhO^-	
metalloporphyrins[a]	1 equiv	3 equiv		1 equiv	3 equiv
free base	+0.35 [H_2O, +2.43]		$P^{2-}/P^{\cdot-}$	+0.06 [PhOH, +1.43]	
Zn^{II}(TPP)	+0.51	+0.49 (+0.24)[b]	+0.80	+0.14	+0.18 (+0.03)[b]
Co^{II}(TPP)	−0.19	−0.22 (+0.19)[b]	+0.80	*c*	*c*
(TPP)$Fe^{III}(ClO_4)$	+0.95[d]	−0.21, +0.95 (+0.49)[b]	+1.15	+0.91	+0.93 (+0.09)[b]
(TDCPP)$Fe^{III}(ClO_4)$	+1.09	−0.10, +1.11, (+0.40)[b]	+1.32	+1.00	+1.04 (+0.03)[b]
(TPP)$Mn^{III}(ClO_4)$	*e*	−0.59, +0.12	+1.26	+0.51	+0.53 (+0.01)[b]

[a] Approximately 0.5 mM. [b] Due to excess base. Potentials other than +0.35 V for free OH^- and +0.06 V for free PhO^- are due to hydrolytic interaction between the base and MeCN. [c] Co^{II}(TPP) is insoluble in MeCN; the addition of PhO^- does not enhance its solubility. [d] (TPP)$Fe^{III}(ClO_4)$ was electrochemically reduced to Fe^{II}(TPP) before ^-OH was added. Peaks are better resolved in the presence of excess ^-OH, but the iron porphyrin is not completely soluble. [e] Greenish white precipitate forms; the addition of 3 equiv of ^-OH to (TPP)$Mn^{III}(ClO_4)$ gives a soluble species.

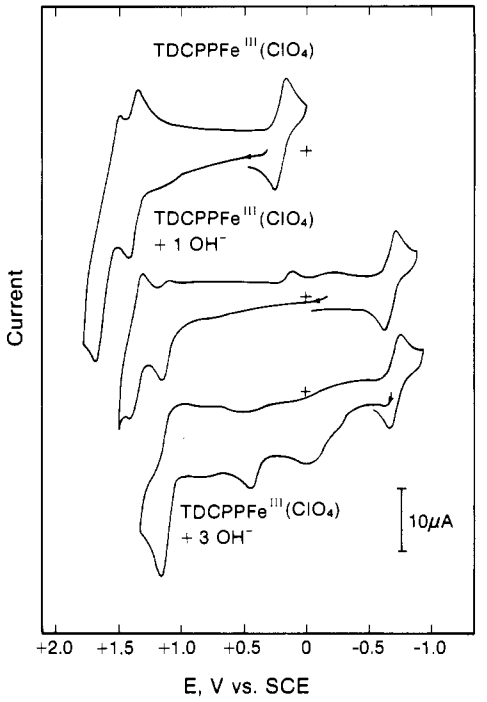

Figure 6. Cyclic voltammograms in MeCN (0.1 M TEAP) of (top) 0.6 mM (TDCPP)$Fe^{III}(ClO_4)$, (middle) 0.6 mM (TDCPP)$Fe^{III}(ClO_4)$ + 1 equiv of (TBA)OH, and (bottom) 0.6 mM (TDCPP)$Fe^{III}(ClO_4)$ + 3 equiv of (TBA)OH [scan rate 0.1 V s^{-1}; GCE (area 0.062 cm^2)].

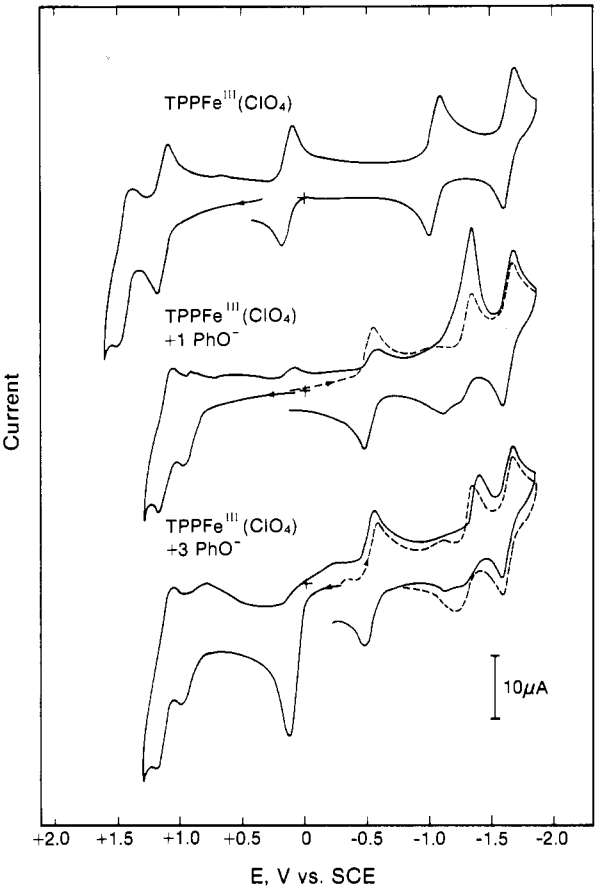

Figure 7. Cyclic voltammograms in MeCN (0.1 M TEAP) of (top) 0.5 mM (TPP)$Fe^{III}(ClO_4)$, (middle) 0.5 mM (TPP)$Fe^{III}(ClO_4)$ + 1 equiv of (TBA)OPh, and (bottom) 0.5 mM (TPP)$Fe^{III}(ClO_4)$ + 3 equiv of (TBA)OPh [scan rate 0.1 V s^{-1}; GCE (area 0.062 cm^2)].

The addition of 1 equiv of ^-OH to (TPP)$Mn^{III}(ClO_4)$ yields a greenish white precipitate, but a clear solution results when a further 2 equiv of ^-OH is added. The anodic voltammogram for the latter solution [after an initial negative scan to reduce manganese(III)] exhibits two new peaks [$E_{1/2}$ = −0.59 V vs SCE (reversible) and +0.12 V (irreversible)]. The peak current for the latter increases linearly with ^-OH concentration for ^-OH: [(TPP)$Mn^{III}(ClO_4)$] mole ratios from 1 up to 9.

The half-wave potentials for the oxidation of ^-OH and PhO^- in the presence of the metalloporphyrins are summarized in Table II.

Discussion and Conclusions

A self-consistent set of redox reactions for the oxidation of ^-OH and PhO^- in the presence of transition-metal complexes is presented in Table III. The oxidation potential for ^-OH in the presence of $Zn^{II}L$ [L = $(OPPh_3)_4$, $(bpy)_3$, TPP^{2-}] and $Y^{III}(OPPh_3)_4^{3+}$ is slightly more positive than that for free ^-OH. This is the anticipated result for the oxidation of ^-OH in the presence of a Lewis acid. The positive metal center delocalizes the electron density of ^-OH to make removal of an electron more difficult; hence, there is a more positive oxidation potential.

The redox potentials for the oxidation of ^-OH, PhO^-, and their adducts with transition-metal complexes are summarized in Table IV. These data indicate that when ^-OH is associated with transition-metal complexes instead of diamagnetic complexes, its oxidation occurs at less positive potentials than that for free ^-OH (despite the Lewis acidities of these complexes). This facilitated oxidation of ^-OH is due to stabilization of the oxidized product ($^{\cdot}OH$) through the formation of a covalent bond between the unpaired p electron of $^{\cdot}OH$ and an unpaired d electron of the metal ion. This phenomenon is analogous to the stabilization observed in the oxidation of dithiolate–metal complexes via covalent d–p bond formation.[11] The extent of this stabilization can be estimated from the negative shift of the oxidation potential for ^-OH oxidation in the presence of $M^{II}L^{2+}$ [M = Mn, Fe, Co, Ni; L = $(OPPh_3)_4$, $(bpy)_3$] relative to that in the presence of $Zn^{II}L^{2+}$. The more negative the oxidation potential, the greater the stabilization and the bond strength. The order of M^{II}–($^{\cdot}OH$) bond strength for L = $(OPPh_3)_4$ is Co (17 kcal)[22] > Ni (16 kcal) > Fe (13 kcal)

(22) Covalent bond energies are approximately equal to $(\Delta E)nF$; for one-electron processes, BE (kcal) = ΔE × 23.1.

Table III. Redox Reactions for Hydroxide Ion and Its Adducts with Transition-Metal Complexes in MeCN (0.1 M TEAP)

Free ^-OH

$$^-OH \xrightarrow{E_{1/2} = +0.35\ V\ vs\ SCE} {}^\bullet OH + e^- \xrightarrow{^-OH} O^{\bullet-} + H_2O \xrightarrow{E_{1/2} < +0.35\ V} O^{2\bullet} + e^-$$

Transition-Metal Complexes (M = Mn, Fe, Co, Ni)

$$Zn^{II}(OPPh_3)_4^{2+} \xrightarrow{^-OH} Zn^{II}(OPPh_3)_4(^-OH)_2 \xrightarrow[^-OH]{+0.63\ V} Zn^{II}(OPPh_3)_4(^-OH)(O^{\bullet-}) + H_2O + e^-$$

$$M^{II}(OPPh_3)_4^{2+} \xrightarrow{^-OH} M^{II}(OPPh_3)_4(^-OH)_2 \xrightarrow[^-OH]{-0.09\ to\ +0.27\ V} (Ph_3PO)_4M^{II}(O^{\bullet-})(^-OH) + H_2O + e^- \xrightarrow{E_{1/2} < -0.09\ to\ +0.27\ V} (Ph_3PO)_4M^{II}(O^{2\bullet})(^-OH)^+ + e^-$$

$$M^{II}(bpy)_3^{2+} \xrightarrow{^-OH} M^{II}(bpy)_3(^-OH)^+ \xrightarrow{-0.03\ to\ +0.33\ V} M^{II}(bpy)_3(^\bullet OH)^{2+} + e^- \xrightarrow{^-OH} M^{II}(bpy)_2(^-OH)_2 + (1/n)[bpy(^\bullet OH)]_n$$

Metalloporphyrins

$Zn^{II}(TPP)$

$$Zn^{II}(TPP) \xrightarrow{^-OH} Zn^{II}(TPP)(^-OH)^- \xrightarrow[^-OH]{+0.49\ V} Zn^{II}(TPP)(O^{\bullet-})^- + H_2O + e^-$$

$$Zn^{II}(TPP) \xrightarrow{PhO^-} Zn^{II}(TPP)(^-OPh)^- \xrightarrow{+0.18\ V} Zn^{II}(TPP) + PhO^\bullet + e^-$$

$Co^{II}(TPP)$

$$Co^{II}(TPP) \xrightarrow{^-OH} (TPP)Co^{II}(^-OH)^- \xrightarrow{-0.22\ V} (TPP)Co^{II}(^\bullet OH) + e^- \xrightarrow{^-OH} (TPP)Co^{II}(O^{\bullet-})^- + H_2O \xrightarrow{E_{1/2} < -0.22\ V} (TPP)Co^{II}(O^{2\bullet}) + e^-$$

[(por)Fe^{III}](ClO_4)

$$(TPP)Fe^{III}(ClO_4) \xrightarrow[-ClO_4^-]{^-OH} (TPP)Fe^{III}(^-OH) \xrightarrow{+0.95\ V} (TPP)Fe^{III}(^\bullet OH)^+ + e^-$$

$$(TPP)Fe^{III}(^-OH) + 2^-OH \xrightarrow{-0.21\ V} (TPP)Fe^{III}(O^{\bullet-})(^-OH)^- + H_2O + e^- \longrightarrow (TPP)Fe^{II}(O^{2\bullet})(^-OH)^- + e^-$$

$$(TPP)Fe^{III}(ClO_4) \xrightarrow[-ClO_4^-]{PhO^-} (TPP)Fe^{III}(^-OPh) \xrightarrow{+0.91\ V} (TPP)Fe^{III}(^\bullet OPh)^+ + e^-$$

$$(TDCPP)Fe^{III}(ClO_4) \xrightarrow[-ClO_4^-]{^-OH} (TDCPP)Fe^{III}(^-OH) \xrightarrow{+1.09\ V} (TDCPP)Fe^{III}(^\bullet OH)^+ + e^-$$

$$(TDCPP)Fe^{III}(^-OH) + 2^-OH \xrightarrow{-0.10\ V} (TDCPP)Fe^{III}(O^{\bullet-})(^-OH)^- + H_2O + e^- \longrightarrow (TDCPP)Fe^{II}(O^{2\bullet})(^-OH)^-$$

$(TPP)Mn^{III}(ClO_4)$

$$(TPP)Mn^{III}(ClO_4) \xrightarrow[-ClO_4^-]{^-OH} (TPP)Mn^{III}(^-OH) \xrightarrow{^-OH,\ -0.59\ V} (TPP)Mn^{III}(O^{\bullet-})(^-OH)^- + e^-$$

$$(TPP)Mn^{III}(O^{\bullet-})(^-OH)^- + 2^-OH \xrightarrow{+0.12\ V} (TPP)Mn^{III}(^-OH) + O_2 + H_2O + 3e^-$$

$$(TPP)Mn^{III}(ClO_4) \xrightarrow[-ClO_4^-]{PhO^-} (TPP)Mn^{III}(^-OPh) \xrightarrow{+0.51\ V} (TPP)Mn^{III}(^\bullet OPh)^+ + e^-$$

Table IV. Redox Potentials for the Oxidation of ^-OH and ^-OPh and of Their Metal Adducts in Acetonitrile

electrode reaction	$E_{1/2}$, V vs NHE[a]
A. $[M^{II}(OPPh_3)_4]^{2+}$ Complexes	
$2^-OH \rightarrow O^{\bullet-} + H_2O + e^-$	+0.59[b]
$(Ph_3PO)_4Zn^{II}(^-OH)_2 + {}^-OH \rightarrow (Ph_3PO)_4Zn^{II}(^-OH)(O^{\bullet-}) + H_2O + e^-$	+0.67[b]
$(Ph_3PO)_4Ni^{II}(^-OH)_2 + {}^-OH \rightarrow (Ph_3PO)_4Ni^{II}(O^{\bullet-})(^-OH) + H_2O + e^-$	−0.01[b]
$(Ph_3PO)_4Co^{II}(^-OH)_2 + {}^-OH \rightarrow (Ph_3PO)_4Co^{II}(O^{\bullet-})(^-OH) + H_2O + e^-$	−0.05[b]
$(Ph_3PO)_4Fe^{II}(^-OH)_2 + {}^-OH \rightarrow (Ph_3PO)_4Fe^{II}(O^{\bullet-})(^-OH) + H_2O + e^-$	+0.12[b]
$(Ph_3PO)_4Mn^{II}(^-OH)_2 + {}^-OH \rightarrow (Ph_3PO)_4Mn^{II}(O^{\bullet-})(^-OH) + H_2O + e^-$	+0.31[b]
B. Metal–Porphyrin Complexes	
$2^-OH \rightarrow O^{\bullet-} + H_2O + e^-$	+0.59
$H_2O \rightarrow HO^\bullet + H^+ + e^-$	+2.67
$(TPP)Zn^{II}(^-OH)^- + {}^-OH \rightarrow (TPP)Zn^{II}(O^{\bullet-})^- + H_2O + e^-$	+0.73
$(TPP)Co^{II}(^-OH)^- + {}^-OH \rightarrow (TPP)Co^{II}(O^{\bullet-})^- + H_2O + e^-$	+0.02
$(TPP)Fe^{III}(^-OH) \rightarrow (TPP)Fe^{III}(^\bullet OH)^+ + e^-$	+1.19
$(TPP)Fe^{III}(^-OH)_2^- + {}^-OH \rightarrow (TPP)Fe^{III}(O^{\bullet-})(^-OH)^- + H_2O + e^-$	+0.03
$(TDCPP)Fe^{III}(^-OH) \rightarrow (TDCPP)Fe^{III}(^\bullet OH)^+ + e^-$	+1.33
$(TDCPP)Fe^{III}(^-OH)_2^- + {}^-OH \rightarrow (TDCPP)Fe^{III}(O^{\bullet-})(^-OH)^- + H_2O + e^-$	+0.14
$(TPP)Mn^{III}(^-OH)_2^- + {}^-OH \rightarrow (TPP)Mn^{III}(O^{\bullet-})(^-OH)^- + H_2O + e^-$	−0.35
$(TPP)Mn^{III}(O^{\bullet-})(^-OH)^- + 2^-OH \rightarrow (TPP)Mn^{III}(^-OH) + O_2 + H_2O + 3e^-$	+0.36
$PhO^- \rightarrow PhO^\bullet + e^-$	+0.30
$PhOH \rightarrow PhO^\bullet + H^+ + e^-$	+1.67
$(TPP)Zn^{II}(^-OPh)^- \rightarrow (TPP)Zn^{II} + PhO^\bullet + e^-$	+0.42
$(TPP)Fe^{III}(^-OPh) \rightarrow (TPP)Fe^{III}(^\bullet OPh)^+ + e^-$	+1.15
$(TDCPP)Fe^{III}(^-OPh) \rightarrow (TDCPP)Fe^{III}(^\bullet OPh)^+ + e^-$	+1.24
$(TPP)Mn^{III}(^-OPh) \rightarrow (TPP)Mn^{III}(^\bullet OPh)^+ + e^-$	+0.75

[a] $E_{NHE} = E_{SCE} + 0.24$ V. [b] Corrected by −0.20 V for the leveling effect of significant levels of residual H_2O.

> Mn (8 kcal) and for L = $(bpy)_3$ is Ni (16 kcal) > Co (15 kcal) > Fe (9 kcal) > Mn (8 kcal).

When 1 equiv of ^-OH is added to $Fe^{II}L^{2+}$ [L = $(OPPh_3)_4$, $(bpy)_3$], there is no current response (Figure 5), which indicates that the ^-OH is coordinated to the metal center to give a cationic species [$Fe^{II}L(^-OH)^+$]. Because the rate of increase in the anodic current from the addition of $(Bu_4N)OH$ to $Fe^{II}(bpy)_3^{2+}$ is half that for free ^-OH or for its addition in the presence of $Fe^{II}(OPPh_3)_4^{2+}$ (Figure 3), it represents a one-electron process and the other two are two-electron processes. In the case of the

$M^{II}(bpy)_3^{2+}$ complexes there is evidence[7,23] that the oxidation product of ^-OH ($^•OH$) forms an adduct species with bipyridine, which precludes subsequent proton abstraction and the removal of a second electron. Thus, the $M^{II}(bpy)_3^{2+}/^-OH$ systems do not have an ECE pathway available and are one-electron processes (Table III).

Because $Zn^{II}(TPP)$ is a neutral species and the iron(III) and manganese(III) porphyrins have a net charge of +1, the electrostatic effect cannot be separated from the stabilization gained from covalent bond formation. Only $Co^{II}(TPP)$ can be properly compared; the –0.7-V shift indicates a d–p covalent bond strength of 16 kcal,[22] which is in close agreement with those of the ($O^{•-}$) adducts of $Co^{II}(OPPh_3)_4^{2+}$ and $Co^{II}(bpy)_3^{2+}$. Because attempts to synthesize $(TPP)Sc^{III}(ClO_4)$ have failed,[24,25] a diamagnetic reference complex is not available to evaluate the extent of stabilization via covalent bond formation for the iron(III) and manganese(III) porphyrins. An alternative is to use the H_2O oxidation potential as a reference point for the facilitated oxidation of ^-OH in neutral systems, e.g., $(TPP)Fe^{III}(OH)$.

Addition of 1 equiv of ^-OH to $(TDCPP)Fe^{III}(ClO_4)$ yields an adduct with an additional anodic peak (Figure 6; $E_{1/2}$ = +1.09 V vs SCE), which is due to the facilitated oxidation of ^-OH to $^•OH$. When a further 2 equiv of ^-OH is introduced, the cyclic voltammogram includes a new anodic peak ($E_{1/2}$ = –0.10 V) as well as an anodic peak for the oxidation of free ^-OH ($E_{1/2}$ = +0.40 V). The new peak is due to the oxidation of bound ^-OH to bound $^•OH$, which is followed by deprotonation via a second ^-OH to give bound $O^{•-}$. This oxidation peak is broad and its area is approximately twice that for the one-electron Fe^{III}/Fe^{II} redox process, which indicates a two-electron ECE process and that the oxidation potential of $O^{•-}$ is less positive than that for ^-OH ($E_{1/2}$ = –0.10 V). The overall process for the oxidation of $(TDCPP)Fe^{III}(ClO_4)$ after the addition of 3 equiv of ^-OH is outlined in Table III.

Support for ligand-centered oxidation is provided by the electrochemical data for PhO^- in the presence of metalloporphyrins. When phenoxide ion is oxidized to $PhO^•$, there is no available proton to be removed by a second PhO^-, which precludes a two-electron ECE process. Thus, addition of excess PhO^- to $(TPP)Fe^{III}(ClO_4)$ yields a solution with one-electron voltammetric oxidation peaks for the excess free PhO^- ($E_{1/2}$ = +0.09 V vs SCE) and for the 1:1 (PhO^-):$(TPP)Fe^{III}(ClO_4)$ adduct ($E_{1/2}$ = +0.91 V).

A noteworthy point for the oxidation of ^-OH in the presence of $(TPP)Mn^{III}(ClO_4)$ is that the oxidation of excess ^-OH occurs at a significantly less positive potential (+0.12 V vs SCE) than that for free ^-OH (or excess ^-OH in the presence of other metalloporphyrins). The absence of any other oxidation process that is attributable to ^-OH when 9 equiv of ^-OH is added and the linear increase in the +0.12-V peak current with ^-OH concentration are consistent with a catalytic process.

In summary, the electrochemical oxidation of ^-OH in the presence of paramagnetic transition-metal complexes is facilitated by formation of a metal d–oxygen p covalent bond; the negative shift of the ^-OH oxidation potential is a measure of the covalent bond energy and the degree of stabilization of the product species ($^•OH$ and $O^{•-}$). Other investigations[8-10] have shown that the oxidation of O-donor ligands can occur prior to that for the metal ion. Analogous to the dithiolate–metal complexes,[11] the oxidized ligand is stabilized by the coupling of the unpaired d electron of the metal with the unpaired p electron of oxidized ligand to give a d–p covalent bond.

With a means to stabilize the oxy radical oxidation product, the oxidation of ^-OH occurs at modest redox potentials. The iron porphyrin results provide evidence that the active forms of cytochrome P-450, compounds I and II of peroxidase, and compound I of catalase have oxidized oxygen species ($O^{2•}$) rather than the proposed[26] high-valent Fe^{IV}–oxo species. The present results indicate that the redox thermodynamics are most consistent with these biological oxidants and O atom transfer agents formulated as

catalase compound I	$(PhO^•)(P^{2-})Fe^{II}(O^{2•})$
peroxidase compound I	$(Imid)(P^{•-})Fe^{II}(O^{2•})^+$
	$\downarrow +e^-$
peroxidase compound II	$(Imid)(P^{2-})Fe^{II}(O^{2•})$
Cyt P-450 activated state	$(RS^•)(P^{2-})Fe^{II}(O^{2•})$

Work is in progress to electrogenerate these reactive intermediates from iron porphyrin/^-OH combinations and to determine their reactivity with organic substrates. Another investigation of the oxidation of ^-OH in the presence of $(TPP)Mn^{III}(ClO_4)$ should provide insight into the character of the intermediates for the manganese catalyst for water oxidation in photosystem II of green-plant photosynthesis.

Acknowledgment. This work was supported by the National Science Foundation under Grant No. CHE 8516247. We thank Dean Rafael Gana of the Catholic University, Santiago, Chile, for the award of a sabbatical leave to Prof. Pablo Cofré, and we thank Dr. Hiroshi Sugimoto of this department for a sample of $(TDCPP)Fe^{III}(ClO_4)$.

(23) Gillard, R. D. *Coord. Chem. Rev.* **1975**, *16*, 67–94.
(24) An aqueous solution of $HClO_4$ was added to a CH_2Cl_2 solution of $[(TPP)Sc]_2O$.[25]
(25) Gouterman, M.; Hanson, L. K.; Khalil, G.-E., Buchler, J. W.; Rohbock, K.; Dolphin, D. H. *J. Am. Chem. Soc.* **1975**, *97*, 3142–3149.
(26) Groves, J. T.; Haushalter, R. C.; Nakamura, M.; Nemo, T. E.; Evans, B. J. *J. Am. Chem. Soc.* **1981**, *103*, 2884.